http://dx.doi.org/10.5012/bkcs.2013.34.1.107

Electroluminescence Characteristics of a New Green-Emitting Phenylphenothiazine Derivative with Phenylbenzimidazole Substituent

Yeonseon Ahn, Da Eun Jang,† Yong-Bum Cha,† Mansu Kim, Kwang-Hyun Ahn,† and Young Chul Kim*

*Department of Chemical Engineering, Kyung Hee University, Gyeonggi-do 446-701, Korea. *E-mail: kimyc@khu.ac.kr*
†Department of Applied Chemistry, Kyung Hee University, Gyeonggi-do 446-701, Korea
Received September 17, 2012, Accepted October 12, 2012

A new green-emitting material with donor-acceptor architecture, 3,7-bis(1'-phenylbenzimidazole-2'-yl)-10-phenylphenothiazine (BBPP) was synthesized and its thermal, optical, and electroluminescent characteristics were investigated. Organic light-emitting diodes (OLEDs) with four different multilayer structures were prepared using BBPP as an emitting layer. The optimized device with the structure of [ITO/2-TNATA (40 nm)/ BBPP (30 nm)/TPBi (30 nm)/Alq3 (10 nm)/LiF (1 nm)/Al (100 nm)] exhibited efficient green emission. Enhanced charge carrier balance and electron mobility in the organic layers enabled the device to demonstrate a maximum luminance of 31,300 cd/m^2, a luminous efficiency of 6.83 cd/A, and an external quantum efficiency of 1.62% with the CIE 1931 chromaticity coordinates of (0.21, 0.53) at a current density of 100 mA/ cm^2.

Key Words : Phenylphenothiazine derivative, Donor-acceptor architecture, Green-emitting OLED

Introduction

π-Conjugated organic materials have been extensively investigated for electronic and optoelectronic applications, such as organic light-emitting diodes (OLEDs),[1-3] organic photovoltaics (OPVs),[4] thin film transistors,[5] and lasers.[6] Due to their easy processability and chemically tunable performance, the organic functional materials have rapidly progressed to compete with inorganic ones.

An internal charge-transfer compound which has the electron-donating (D) and electron-accepting (A) groups through a π-conjugated linker is one of the most important materials. In the molecules with D-A architecture, the D moiety facilitates hole injection and transport, and the A moiety facilitates electron injection and transport, which enables them to be employed as emitting materials in OLEDs with high efficiency.[7,8]

The structure of π-conjugated D-A molecules and their optical and electrochemical properties could be easily tuned by appropriate chemical modification over a wide range. Electron-deficient benzene-fused five-membered heteroaromatic rings with nitrogen atom such as benzimidazoles have been effectively used as acceptor moieties in the organic materials because of their high thermal, chemical, thermo-oxidative, environmental, and photochemical stabilities, as well as their strong electron-accepting character.[9-11] Furthermore, the heteroaromatic rings are directly boned to a donor to facilitate maximal coplanarity between the donor and the acceptor, which is crucial for the efficient charge transfer in the molecules.[12] Phenothiazines have been intensively investigated as a donor in electrogenerated chemiluminescence (ECL) systems, because of their highly stable radical cations, unique nonplanar geometry, and low reversible oxidation potential.[13,14] The studies of OLEDs based on phenothiazine-containing D-A molecules have already been reported.[7,15] The previous work in our group has demonstrated that phenothianzine and benzimidazole are a good D-A pair for OLEDs.[16,17]

In this work, we report the synthesis of a D-A molecule based on phenylphenothiazine as a donor and phenylbenzimidazole as an acceptor. Also we fabricated green-emitting OLED devices using the new material as an emitting layer and characterized the performance of the devices with different structures.

Experimental

Synthesis. The ^{1}H NMR and ^{13}C NMR spectra were recorded on a Jeol FT-NMR (JNM-AL300) spectrometer at 300 and 75 MHz, respectively. Chemical shifts (multiplicity, coupling constant (Hz), integrated) are referenced to tetramethylsilane (TMS). The high resolution mass spectra were recorded on a Jeol JMS-700 spectrometer. Most of the reagents were obtained from Aldrich.

10-Phenylphenothiazine (2). The phenothiazine (1.0 g, 5.02 mmol) in 50 mL of dimethylformamide (DMF) reacted with iodobenzene (0.62 mL, 27.6 mmol) using literature procedure to give 10-phenylphenothiazine (**2**) (1.08 g, 3.92 mmol, 78%).[18] mp 95 °C; ^{1}H NMR (300 MHz, $CDCl_3$) δ 7.57-7.52 (m, 2H), 7.45-7.40 (m, 1H), 7.36-7.33 (m, 2H), 7.00-6.95 (m, 2H), 6.83-6.74 (m, 4H), 6.17 (d, J = 7.73 Hz, 2H); ^{13}C NMR (75 MHz, $CDCl_3$) δ 142.59, 139.22, 129.23, 129.12, 126.57, 125.20, 125.08, 120.83, 118.44, 114.36.

10-Phenylphenothiazine-3,7-dicarbaldehyde (3). The Vilsmeier-Haak reaction[17] of 10-phenylphenothiazine (**2**) (1.0 g, 3.63 mmol) with phosphorus(V) oxychloride (13.3 mL, 145 mmol) and DMF (11.2 mL, 145 mmol) in 1,2-dichloroethane (5 mL) formed 10-phenylphenothiazine-3,7-

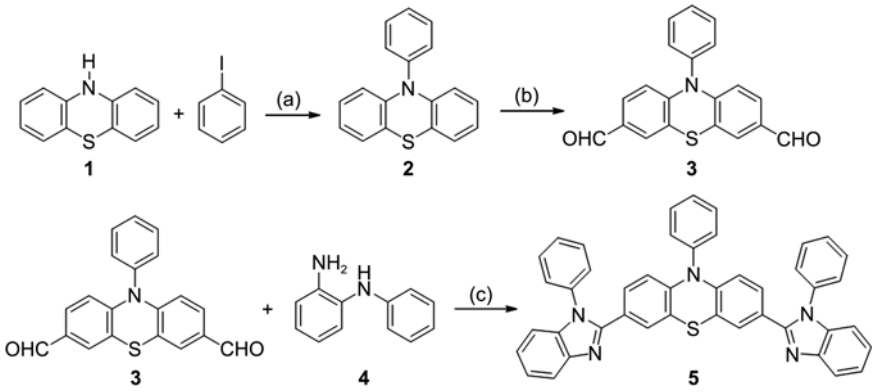

Scheme 1. Synthesis of 3,7-bis(1'-phenylbenzimidazole-2'-yl)-10-phenylphenothiazine (BBPP, **5**). Reagents and conditions; (a) iodobenzene, copper powder, K_2CO_3, DMF, reflux; (b) phosphorus(V) oxychloride, DMF, 1,2-dichloroethane, reflux; (c) $Na_2S_2O_5$, DMF, reflux.

dicarbaldehyde **3** (0.85 g, 2.56 mmol, 71%). mp 145 °C; ^{1}H NMR (300 MHz, $CDCl_3$) δ 9.54 (s, 2H), 7.89 (d, J = 8.22 Hz, 1H), 7.50-6.97 (m, 7H), 6.75-6.72 (m, 1H), 5.96-5.94 (d, J = 8.43 Hz, 2H); ^{13}C NMR (75 MHz, $CDCl_3$) δ 191.0, 148.1, 143.4, 138.7, 134.9, 129.8, 129.3, 129.2, 128.2, 127.9, 126.3, 40.4.

3,7-Bis(1-phenylbenzimidazol-2-yl)-10-phenylphenothiazine (5, BBPP). BBPP was prepared by the oxidative coupling of 10-phenylphenothiazine-3,7-dicarbaldehyde (**3**) (0.4 g, 1.21 mmol) with *N*-phenyl-1,2-phenylenediamine (**4**) (0.49 g, 2.66 mmol) under the treatment of sodium metabisulfite (0.58 g, 3.03 mmol).[17] After purification by chromatography (silica gel, hexane/acetone = 2:1), **5** was obtained in 80% yield (0.64 g, 0.97 mmol) as a yellow solid. mp 297 °C; ^{1}H NMR (300 MHz, $CDCl_3$) δ 7.85-7.82 (s, 2H), 7.61-7.45 (m, 9H), 7.40-7.37 (m, 1H), 7.33-7.27 (m, 10H), 7.23-7.16 (m, 3H), 6.81 (d, J = 8.6 Hz, 2H), 5.88 (s, 2H); ^{13}C NMR (75 MHz, $CDCl_3$) δ 151.11, 144.24, 139.78, 137.24, 136.87, 131.04, 130.81, 130.03, 128.81, 128.72, 127.80, 127.45, 127.38, 123.96, 122.96, 119.44, 115.02, 110.26. EI-HRMS (70 eV) *m/z* calcd for $C_{44}H_{29}N_5S$ 659.2144, found 659.2221.

Measurement. Thermogravimetric analysis (TGA) and differential scanning calorimetry (DSC) measurement of BBPP were carried out on a TA Instrument model SDT Q600 and a Perkin Elmer DSC N536-0003, respectively, in nitrogen at a scan rate of 10 °C/min. UV-Vis absorption spectra were recorded on an Agilent 8453 spectrophotometer and the photoluminescence (PL) spectra were obtained using a PTI QM-4 spectrofluorometer. The highest occupied molecular orbital (HOMO) energy level of BBPP was measured by using an eDAQ e-corder 401 cyclic voltammeter (CV) in dichloromethane (DCM) with a glassy carbon working electrode, a platinum auxiliary electrode, and a saturated Ag/AgCl reference electrode in 0.1 M $TBAPF_6$ (tetrabutylammonium hexafluorophosphate) as a supporting electrolyte (scan rate: 50 mV/s). The current density-voltage-luminance (J-V-L) characteristics of the OLED devices were measured with a JBS IVL-300 EL characterization system equipped with a Keithley 2400 sourcemeter.

Fabrication of OLEDs. We fabricated four types of OLED devices with BBPP as an emitting layer (see Figure 1). *N,N′*-Bis(naphthalen-1-yl)-*N,N′*-bis(phenyl)benzidine (NPB) or 4,4',4"-tris(2-naphthyl(phenyl)amino)triphenylamine (2-TNATA) was used as a hole transport layer and 2,9-dimethyl-4,7-diphenyl-1,10-phenanthroline (BCP) served as a hole blocking and electron transport layer. 1,3,5-Tris(*N*-phenylbenzimidizol-2-yl)benzene (TPBi) was also tested as a hole blocking and electron transport layer with an electron injection layer of tris-(8-hydroxyquinoline) aluminum (Alq3). The bilayer of lithium fluoride (LiF) and aluminum (Al) was used as a cathode in all OLED devices. ITO-coated glass substrates with a surface resistance of 10 Ω/sq was patterned by photolithography and cleaned with trichloroethylene, acetone, deionized water, and isopropyl alcohol in an ultrasonic bath, and then dried in a convection oven at 120 °C. The cleaned ITO surface was oxygen plasma-treated to improve adhesion with organic materials. All organic and metal layers were deposited by thermal evaporation under

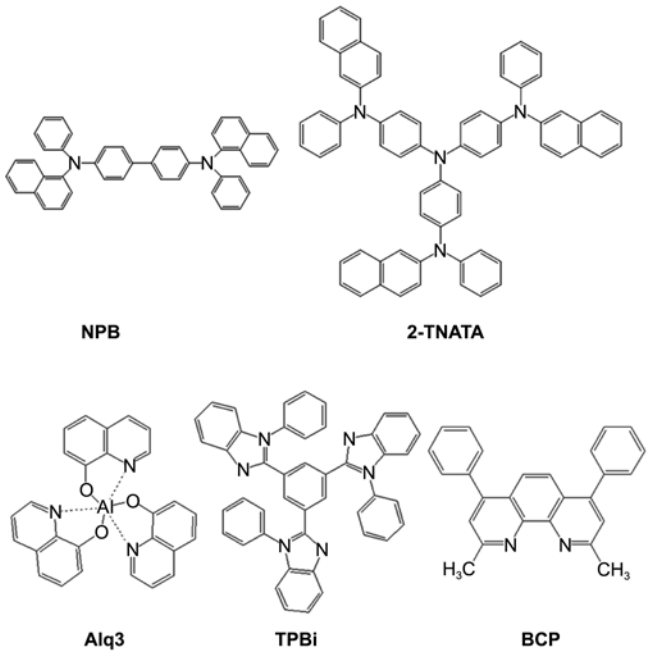

Figure 1. Chemical structures of the materials used in the OLED devices fabrication.

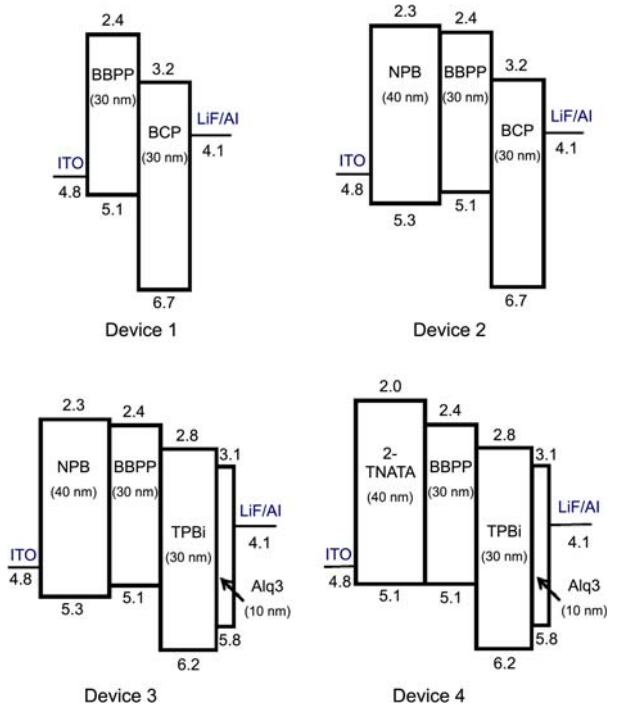

Figure 2. Device structures and energy level diagrams of the OLEDs tested in this work.

2×10^{-6} torr on the ITO substrate and the deposition rates were 1.0, 0.1, 3-4 Å/s for the organic, LiF, and Al layers, respectively. Active emitting area of the OLED devices was patterned to be 3×3 mm^2.

Results and Discussion

Thermal Properties of BBPP. Thermal stability and crystallizability of BBPP were examined by TGA and DSC, respectively. The thermal decomposition temperature (T_d) of BBPP, defined as the temperature of 5% weight loss, was measured to be 419 °C, which is much higher than the thermal evaporation process temperature of the material (270 °C). The DSC thermograms showed that BBPP has a T_g of 145 °C and a T_m of 263 °C during the first heating scan, however, no recrystallization and melting was observed during the subsequent cooling and second heating scans at 10 °C/min, which means BBPP is hardly crystallizable by the Joule heating during the device operation, especially at high current densities.

Optical Properties and Orbital Energy Levels of BBPP. The highest occupied molecular orbital (HOMO) energy level of BBPP was estimated to be 5.15 eV from the onset of the oxidation peak on its cyclic voltammogram.[19] Also the lowest unoccupied molecular orbital (LUMO) energy level could be calculated by the equation; $E_{LUMO} = E_{HOMO} -$ Bandgap energy (E_g). Where, the bandgap energy was estimated to be 2.69 eV from the onset of the optical absorption spectrum (460 nm) of a dilute BBPP solution in DCM ($\sim 10^{-5}$ M) shown in Figure 3, by using the relationship; E_g (eV) = $1240/\lambda_{onset}$. Figure 3 also demonstrates that BBPP

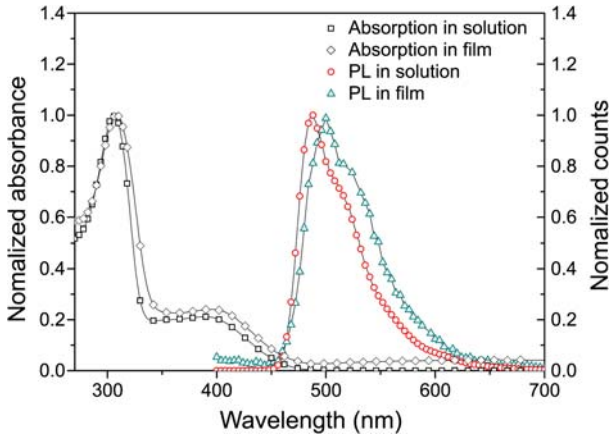

Figure 3. UV-vis absorption and photoluminescence (PL) spectra of BBPP in dilute DCM solution ($\sim 10^{-5}$ M) and vacuum-deposited solid film.

Table 1. Thermal and optical properties, and orbital energy levels of BBPP

Thermal properties		T_g (°C)	145
		T_m (°C)	263
		T_d (°C)	419
Optical properties	UV	$\lambda_{max, abs}$	305, 389
		$\lambda_{onset, abs}$	460
	PL	$\lambda_{max, PL}$ in film (nm)	502
		$\lambda_{max, PL}$ in solution (nm)	488
Orbital energy levels		HOMO (eV)	5.15
		LUMO (eV)	2.46
		Bandgap (eV)	2.69

gives a green photoluminescence (PL) with emission wavelengths ranging from 450 to 650 nm, however, the peak wavelength was 488 nm for the dilute solution while 502 nm for the thin solid film vacuum-deposited on a quartz substrate. The solution PL peak blue-shifted about 20 nm compared with the solid PL because of the dilution effect in a polar surrounding solvent.[20] A large Stokes shift, a large separation between the peak wavelengths of the optical absorption and the PL emission, was observed, which can help to enhance the emission efficiency by preventing the self-absorption of the emitted light.[21]

Electroluminescence Properties of BBPP. To evaluate the potential of BBPP as an emitting material with the electron donor-acceptor structure based on phenylphenothiazine and phenylbenzimidazole, we prepared the simplest device (device 1) using 2,9-dimethyl-4,7-diphenyl-1,10-phenanthroline (BCP) as an electron injection and transport layer. Also BCP was expected to serve as a hole blocking layer to confine the exciton formation inside the BBPP emitting layer and balance the charge injection. Device 1 gave a green EL emission spectrum peaking at 500 nm (Figure 4) with the Commission International d'Eclairage (CIE) coordinates of (0.23, 0.51), which is identical to the thin-film PL emission spectrum of BBPP shown in Figure 3. The relatively low turn-on voltage (6.2 V at 100 cd/m^2) and

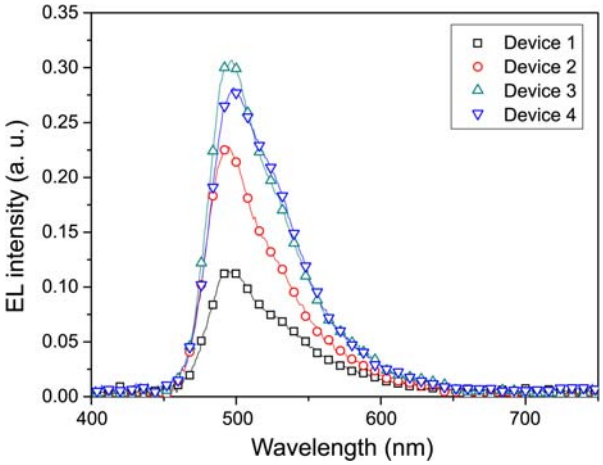

Figure 4. Electroluminescence spectra of the OLED devices prepared using BBPP as an emitting layer, obtained at a current density of 100 mA/cm^2.

high maximum brightness (13,700 cd/m^2) of the simplest device, device 1, demonstrated the D-A character of BBPP facilitating the charge carriers injection and transport. However, device 1 gave a low luminous efficiency of 3.03 cd/A and an external quantum efficiency (EQE) of 0.78% at 100 mA/cm^2. This is attributed to poor charge carriers harvest in the device leaving a considerable amount of injected holes and electrons passing through the device without recombination. The performance of device 1 can generally be improved by using an additional layer of hole transport material such as *N,N'*-bis(naphthalen-1-yl)-*N,N'*-bis(phenyl)benzidine (NPB). When a 40 nm-thick NPB layer was inserted between BBPP and the anode as in device 2, the device could be operated at lower voltages and the maximum brightness increased to 23,700 cd/m^2. Both the luminous efficiency and the EQE of device 2 were improved to 5.72 cd/A and 1.31% at 100 mA/cm^2, respectively, probably resulting from the enhanced hole injection and higher hole transport mobility of NPB.

Further improvements were achieved by incorporating a 30 nm-thick 1,3,5-tris(*N*-phenylbenzimidizol-2-yl)benzene (TPBi) layer for hole blocking and electron transport, and a 10 nm-thick tris-(8-hydroxyquinoline) aluminum (Alq3) layer for electron injection, resulting in a maximum brightness of 34,800 cd/m^2 and a EQE of 1.43% at 100 mA/cm^2 with a luminous efficiency of 6.42 cd/A in device 3. Alq3 and TPBi have higher electron mobility of 7.2×10^{-6} and 8×10^{-5} cm^2/Vs,[22] respectively, than BCP (5.6×10^{-6} cm^2/Vs). This result suggests that the high electron mobility of those materials helped to improve the charge carrier balance in the emitting layer to increase the device efficiency. After

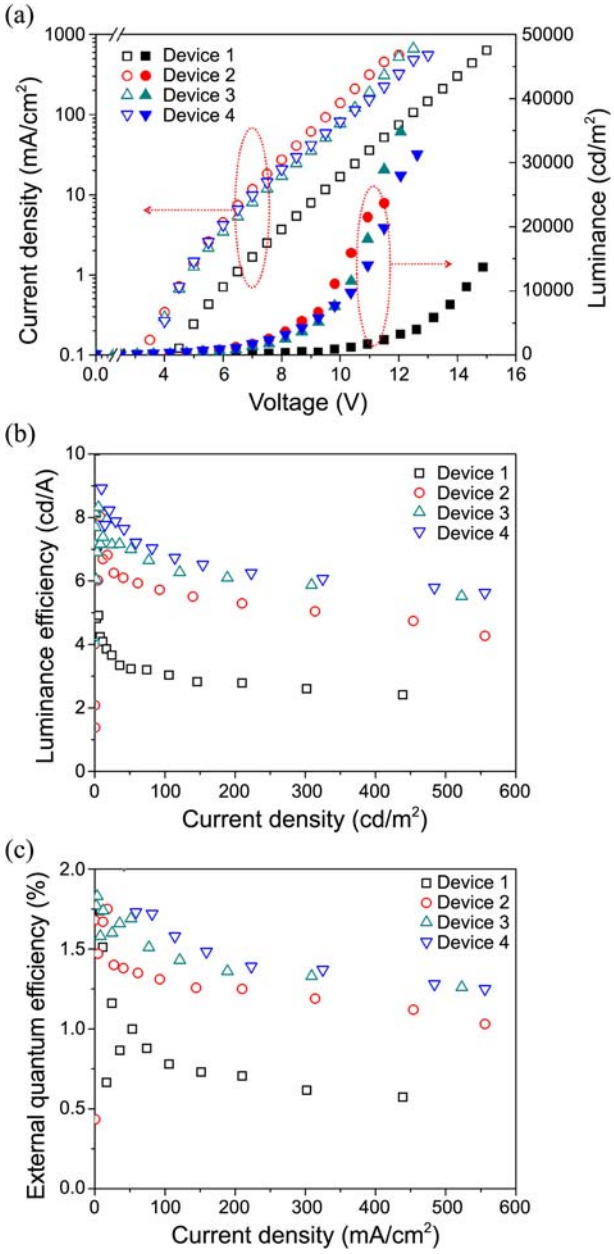

Figure 5. Characteristics of the OLED devices with four different structures; (a) Luminance and current density vs applied voltage; (b) Luminous efficiency vs current density; (c) External quantum efficiency *vs* current density.

Table 2. Electroluminescence characteristics of the OLED devices

	Turn-on voltage (V)[a]	L_{max} (cd/m^2)	η_L (cd/A)[b]	η_{ext} (%)[b]	CIE coordinates [x,y][b]	$\lambda_{max, EL}$ (nm)
Device 1	6.2	13,700	3.03	0.78	0.23, 0.51	500
Device 2	4.4	23,700	5.72	1.31	0.21, 0.51	494
Device 3	5.1	34,800	6.42	1.43	0.21, 0.53	496
Device 4	4.0	31,300	6.83	1.62	0.21, 0.53	497

[a]Measured at 100 cd/m^2. [b]Measured at 100 mA/cm^2

optimizing the electron injection and transport layers, we employed 4,4',4"-tris(2-naphthyl(phenyl)amino)triphenylamine (2-TNATA) as the hole transport layer (HTL) instead of NPB. Device 4 featuring an HTL of 2-TNATA showed lower current density than those of device 2 and device 3 featuring a HTL of NPB, because the hole mobility of 2-TNATA (6.3×10^{-5} cm^2/Vs) is lower than that of NPB (1.6×10^{-3} cm^2/Vs).

Even at lower current densities, device 4 demonstrated the highest luminous efficiency of 6.83 cd/A and EQE of 1.62% at 100 mA/cm^2. For most OLED devices, electrons are deficient in the emitting layer because of the relatively high electron injection barrier and low electron mobility in organic materials. It appears that using an HTL with a lower hole mobility could enhance the charge carrier balance and recombination efficiency for exciton generation, to give a better emission efficiency. These results demonstrate that optimization of the charge carrier balance is very important for extracting the maximum EL efficiency from a given emitting material. EL performances of the OLED devices investigated in this work are summarized in Table 2.

Conclusion

3,7-Bis(1'-phenylbenzimidazole-2'-yl)-10-phenylphenothiazine (BBPP) was synthesized to have a donor-acceptor architecture of phenylphenothiazine and phenylbenzimidazole moieties. After examining the thermal and optical properties as well as the HOMO and LUMO energy levels, BBPP was employed as an emitting layer of OLED devices and the device structure was optimized to give the highest luminous efficiency. The multilayer OLED device prepared using 2-TNATA as a hole transport layer with TPBi and Alq3 as an electron transport layer and an electron injection layer, respectively, gave the most efficient green emission. This device demonstrated a maximum luminance of 31,300 cd/m^2, a maximum luminance of of 6.83 cd/A, and an external quantum efficiency of 1.62% with the CIE 1931 chromaticity coordinates of (0.21, 0.53) at 100 mA/cm^2, showing a better efficiency than the device using NPB as a hole transport layer although NPB has a higher hole mobility. These results confirm that balanced charge carrier injection and high recombination efficiency is essential for extracting the maximum EL efficiency from a given emitting material.

Acknowledgments. This research was supported by Basic Science Program through the National Research Foundation of Korea (NRF) funded by the Ministry of Education, Science and Technology (Grant No. 2011-0027256).

References

1. Tang, C. W.; Vanslyke, S. A. *Appl. Phys. Lett.* **1987**, *51*, 913.
2. Meyer, J.; Hamwi, S.; Bulow, T.; Johanes, H.-H.; Riedl, T.; Kowalsky, W. *Appl. Phys. Lett*. **2007**, *91*, 113506.
3. Yang, Q.; Hao, Y.; Wang, Z.; Li, Y.; Wang, H.; Xu, B. *Synthetic Metals* **2012**, *162*, 398.
4. Kim, C.; Choi, H.; Kim, S.; Baik, C.; Song, K.; Kang, M.-S.; Kang, S.-O.; Ko, J. *J. Org. Chem.* **2008**, *73*, 7072.
5. Dimitrakopoulos, C. D.; Malenfant, P. R. L. *Adv. Mater.* **2002**, *14*, 399.
6. Tessler, N. *Adv. Mater.* **1999**, *11*, 363.
7. Kulkarni, A. P.; Kong, X.; Jenekhe, S. A. *Adv. Funct. Mater.* **2006**, *16*, 1057.
8. Wang, R. Y.; Jia, W.-L.; Aziz, H.; Vamvounis, G.; Wang, S.; Hu, N.-X.; Popovic, Z. D.; Coggan, J. A. *Adv. Funct. Mater.* **2005**, *15*, 1483.
9. Ozelcaglayan, A. C.; Sendur, M.; Akbasoglu, N.; Apaydin, D. H.; Cirpan, A.; Toppare, L. *Electrochimica Acta* **2012**, *67*, 224.
10. Wang, H.-H.; Wu, S.-P. *J. Appl. Polym. Sci.* **2003**, *90*, 1435.
11. Wang, S.; Zhou, H; Dang, G.; Chen, C. *J. Polym. Sci. Part A: Polymer Chemistry* **2009**, *47*, 2024.
12. Kannan, R.; He, G. S.; Yuan, L.; Xu, F.; Prasad, P. N.; Dombroskie, A. G. *Chem. Mater*. **2001**, *13*, 1896.
13. Jenekhe, S. A.; Lu, L.; Alam, M. M. *Macromolecules* **2001**, *34*, 7315.
14. Weiss, E. A.; Tauber, M. J.; Kelley, R. F.; Ahrens, M. J.; Ratner, M. A.; Wasielewski, M. R. *J. Am. Chem. Soc.* **2005**, *127*, 11842.
15. Sun, X.; Liu, Y.; Xu, X.; Yang, C.; Yu, G.; Chen, S.; Zhao, Z.; Qiu, W.; Li, Y.; Zhu, D. *J. Phys. Chem. B* **2005**, *109*, 10786.
16. Lee, S.-H.; Kim, M. S.; Cha, Y.-B.; Ahn, K.-H.; Kim, Y. C. *Mol. Cryst. Liq. Cryst.* **2010**, *520*, 36.
17. Zhang, X.-H.; Kim, S. H.; Lee, I. S.; Gao, C. J.; Yang, S. I.; Ahn, K.-H. *Bull. Korean. Chem. Soc.* **2007**, *28*, 1389.
18. Li, D.; Ren, J.; Li, J.; Wang, Z.; Bo, G. *Dyes and Pigments* **2001**, *49*, 181.
19. Lee, H.; Kim, J. H. *Polymer Science and Technology* **2007**, *18*, 488.
20. Zhang, X.; Wu, Z.; Wang, D.; Wang, D.; Hou, X. *J. Appl. Polym. Sci.* **2010**, *15*, 1213.
21. Peng, X.; Song, F.; Lu, E.; Wang, Y.; Zhou, W.; Fan, J.; Gao, Y. *J. Am. Chem. Soc.* **2005**, *127*, 4170.
22. Tao, Y.; Yang, C.; Qin, J. *Chem. Soc. Rev.* **2011**, *40*, 2943.